Bone. Author manuscript; available in PMC: 2014 Dec 1.
Published in final edited form as: Bone. 2013 Sep 19;57(2):10.1016/j.bone.2013.09.003. doi: 10.1016/j.bone.2013.09.003

Chronic Skeletal Unloading of the Rat Femur: Mechanisms and Functional Consequences of Vascular Remodeling

John N Stabley [1], Rhonda D Prisby [2], Bradley J Behnke [1], Michael D Delp [1]

Author information Article notes Copyright and License information

PMCID: PMC3856860 NIHMSID: NIHMS526040 PMID: 24056176

Abstract

Chronic skeletal unloading diminishes hindlimb bone blood flow. The purpose of the present investigation was to determine 1) whether 7 and 14 days of skeletal unloading alters femoral bone and marrow blood flow and vascular resistance during reloading, and 2) whether putative changes in bone perfusion are associated with a gross structural remodeling of the principal nutrient artery (PNA) of the femur. Six-month old male Sprague-Dawley rats were assigned to 7-d or 14-d hindlimb unloading (HU) or weight-bearing control groups. Bone perfusion was measured following 10 min of standing (reloading) following the unloading treatment. Histomorphometry was used to determine PNA media wall thickness and maximal diameter. Bone blood flow, arterial pressure and PNA structural characteristics were used to calculate arterial shear stress and circumferential wall stress. During reloading, femoral perfusion was lower in the distal metaphyseal region of 7-d HU rats, and in the proximal and distal metaphyses, diaphysis and diaphyseal marrow of 14-d

HU animals relative to that in control rats. Vascular resistance was also higher in all regions of the femur in 14-d HU rats during reloading relative to control animals. Intraluminal diameter of PNAs from 14-d HU rats (138 ± 5 μm) was smaller than that of control PNAs (162 ± 6 μm), and medial wall thickness was thinner in PNAs from 14-d HU (14.3 ± 0.6 μm) versus that of control (18.0 ± 0.8 μm) rats. Decreases in both shear stress and circumferential stress occurred in the PNA with HU that later returned to control levels with the reductions in PNA maximal diameter and wall thickness, respectively. The results demonstrate that chronic skeletal unloading attenuates the ability to increase blood flow and nutrient delivery to bone and marrow with immediate acute reloading due, in part, to a remodeling of the bone resistance vasculature.

Keywords: Bone Blood Flow, Hindlimb Unloading, Vascular Resistance

INTRODUCTION

The chronic unloading of the skeleton, such as occurs with prolonged bedrest and microgravity, induces a number of alterations to bone, including reductions in bone mass, density, mineralization, trabecular thickness and osteoblastic activity [1–4]. Despite the critical role the microcirculation plays in the maintenance of bone interstitial fluid pressure and flow [5–8], osteoblast and osteoclast progenitor cell transport [9, 10], and the putative coupling of bone perfusion and vascular signaling to bone remodeling [6, 9, 11–15], few studies in the literature have examined the effects of chronic unloading on the skeletal vasculature. Fei et al. [17] have reported small vessel rarefaction in the tibia of hindlimb unloaded (HU) rats, but the effects of unloading on the bone resistance vasculature, the site of control of bone and marrow perfusion, are unknown.

In human models of skeletal unloading, disuse osteopenia occurs at sites where hydrostatic pressure is reduced [7, 18, 19]. Likewise, in patients with unilateral lower limb arterial disease, reductions in blood flow to the affected limb are associated with decrements in femoral bone mineral density [20]. In HU rats, bone loss also occurs in skeletal sites where arterial pressure and perfusion are diminished [1, 6]. Although reductions in both arterial pressure and blood flow have been previously shown to induce vascular remodeling of large conduit arteries [21–24] and resistance arteries in skeletal muscle [25], no studies have examined the impact of altered microvascular hemodynamics on resistance artery structure in bone. Therefore, the purpose of the present investigation was to determine, 1) whether vascular remodeling occurs in the principal nutrient artery (PNA) of the rat femur during skeletal unloading, 2) whether alterations in PNA circumferential wall stress or intraluminal shear stress are regulated variables when putative changes in vascular structure occur, and 3) whether possible changes in vascular structure are associated with alterations in bone and marrow perfusion with reloading. We hypothesized that the unloading-induced reductions in hindlimb arterial pressure would diminish PNA circumferential wall stress while reductions in blood flow to the femur would reduce PNA intraluminal shear stress. Further, reductions in these mechanical stresses would be normalized through decreases in PNA medial wall thickness and intraluminal diameter, respectively. Additionally, we hypothesized that the shear stress-induced reductions in PNA intraluminal diameter would be associated with a diminished bone hyperemia with skeletal

reloading.

METHODS

Animals

All procedures performed in this study were approved by the University of Florida and the Texas A&M University Institutional Animal Care and Use Committees and conformed to the National Institutes of Health (NIH) *Guide for the Care and Use of Laboratory Animals* (Eighth edition, 2011).

Six-month-old male Sprague-Dawley rats (n = 49) were obtained from Harlan (Houston, TX) and individually housed in a temperature-controlled (23 ± 2 °C) room with a 12:12 hr light-dark cycle. Water and rat chow were provided *ad libitum*. Animals were randomly assigned to either a normal weight-bearing control (Con) group or 7-d and 14-d hindlimb unloaded (HU) groups. The animals were further subdivided into groups for blood flow (Con, n = 13; 7-d HU, n = 11; 14-d HU, n = 11) and arterial morphology (Con, n = 7; 14-d HU, n = 7) determination. The hindlimbs of the HU groups were elevated to an approximate spinal angle of ~40° via orthopedic traction tape placed around the proximal two-thirds of the tail in a modification of techniques previously described [6, 25, 26]. The height of the hindlimb elevation was adjusted to prevent the hindlimbs from touching supportive surfaces while the forelimbs maintained contact with the cage floor. This configuration allowed free range of movement around the cage while unloading the hindlimb skeleton. HU animals were kept in this position for a period of 7 or 14 d. Control animals were individually maintained in their normal cage environment.

Bone Blood Flow Determination

Surgical Procedures

Control and 7-d and 14-d HU rats were anesthetized with pentobarbital sodium (30 mg/kg ip). HU rats were anesthetized while remaining in the unloaded position to avoid any weight-bearing activity. A catheter (Dow Corning, Silastic; ID 0.6 mm, OD 1.0 mm) filled with heparinized (200 U/ml) saline was advanced into the ascending aorta via the right carotid artery as previously described [6, 26]. This catheter was subsequently used for the infusion of radiolabeled microspheres to measure blood flow. A second polyurethane catheter (Braintree Scientific, Micro-renathane; ID 0.36mm, OD 0.84 mm), used for the withdrawal of a reference blood sample and measurement of hindlimb arterial pressure, was implanted in the caudal artery of the tail and filled with heparinized saline as previously described [6, 26, 27]. Both catheters were externalized and secured on the dorsal cervical region.

Experimental Protocol

Following 24 hr of recovery from the surgical procedure, Con and HU animals were instrumented for blood flow determination. Blood flow in the Con group was first measured while the animals were hindlimb unloaded by elevating their hindlimbs to an approximate spinal angle of ~40° for 10 min. The animals were then returned to a normal standing position for 10 min and a second blood flow measure was made using different radiolabeled microspheres. In the HU groups, blood flow was first measured while the animals were in the unloaded position. The rats' hindlimbs were then lowered to a weight-bearing standing position and blood flow was again measured following 10 min of standing. After the microsphere infusions, euthanasia solution (0.4 ml/kg; Euthanasia-5 Solution, Henry Schein Inc.) was infused through the carotid catheter. Femora and soleus muscles were removed from the carcass. The soleus muscle was weighed to determine the efficacy of the unloading treatment. Femora from both hindlimbs were sectioned into three regions, the proximal and distal metaphyses and diaphysis; the femoral marrow was removed from the diaphysis and counted as a fourth region as previously described [6, 12, 15]. Corresponding femoral sections from the left and right hindlimbs were combined for each animal to ensure sufficient microspheres in the samples. Bone samples were weighed and placed in counting vials for flow determination. Mass of the femoral marrow was determined by weighing the shaft before and after the marrow was removed.

Blood Flow and Vascular Resistance

Radiolabeled (^{85}Sr, ^{113}Sn, and ^{46}Sc) microspheres (Perkin Elmer) with a 15 μm diameter were used for blood flow measurements as previously described [6, 12, 15, 26]. The 15 μm diameter of the microspheres results in the spheres being trapped in small arterial vessels upstream of capillaries, and therefore reflects flow through the arteries. Radioactivity of the samples was measured with a gamma counter (Packard AutoGamma 5780) and flows were computed (PC-GERDA V2.9 Software) from counts per minute and tissue wet weights. Vascular resistance was calculated by dividing arterial pressure by tissue blood flow.

Central Hemodynamics

Electronically averaged mean arterial pressure and heart rate (pulse pressure rate) were recorded from the caudal catheter immediately before and after each microsphere infusion and averaged.

Arterial Morphology Determination

Microvessel Preparation

At the end of the experimental period, Con and 14-d HU rats were injected with euthanasia solution (0.5 ml/kg ip; Euthanasia-5 Solution, Henry Schein Inc.). The hindlimbs were removed from the carcass and placed in a 4°C filtered physiological saline buffer solution (PSS). Using a stereomicroscope, the femoral PNA was identified. In the area where the PNA entered the femoral diaphysis, muscle fibers surrounding the bone and PNA were carefully dissected away (Fig 1). The femoral diaphysis was then cut adjacent to the nutrient foramen and canal using a small bone saw, taking care not to penetrate the canal with the saw blade. The femur was then carefully broken along the cuts and the length of the PNA from the periosteal surface into the marrow was isolated and transferred to a Lucite vessel chamber containing PSS. One end of the PNA was cannulated with a glass micropipette filled with filtered PSS solution and tied securely to the pipette with 11-0 ophthalmic suture (Alcon Laboratories, Inc., Fort Worth, TX). The other end of the vessel was cannulated with a second micropipette and secured with suture as previously described [12, 15, 16]. Intraluminal pressure in the isolated PNA was set at 44 mmHg (60 cmH_2O) with two hydrostatic pressure reservoirs. This intravascular pressure was selected based on previously reported intravascular pressures of 43 ± 1.8 mmHg and 46 ± 2.6 mmHg in skeletal muscle resistance arteries of similar size to the PNA in normotensive rats [28]. The distance between the cannulating micropipettes was adjusted so that the PNA axial length was straight but not stretched. The vessel chamber and pressure lines were then filled with calcium-free PSS containing 2.0 mM EDTA. PNAs were rinsed every 15 min during a 60 min period to facilitate complete relaxation of the vascular smooth muscle cells. During the last 15-min period, the vasodilator sodium nitroprusside (10^{-4} M) was added to the vessel chamber to ensure complete relaxation of the vascular smooth muscle. Maximal intraluminal diameter and medial wall thickness were first determined at the end of this second 15-min incubation using videomicroscopic techniques [29–31]. Maximal intraluminal diameter and medial wall thickness were taken as the mean of three separate measurements from positions randomly selected along the PNA length. To measure medial wall thickness, the video caliper was positioned on the outer and inner surface of the medial layer of the vessel. The focal plane was adjusted through the medial wall and the smallest distance between the inner and outer surface was taken to be medial wall thickness.

Figure 1.

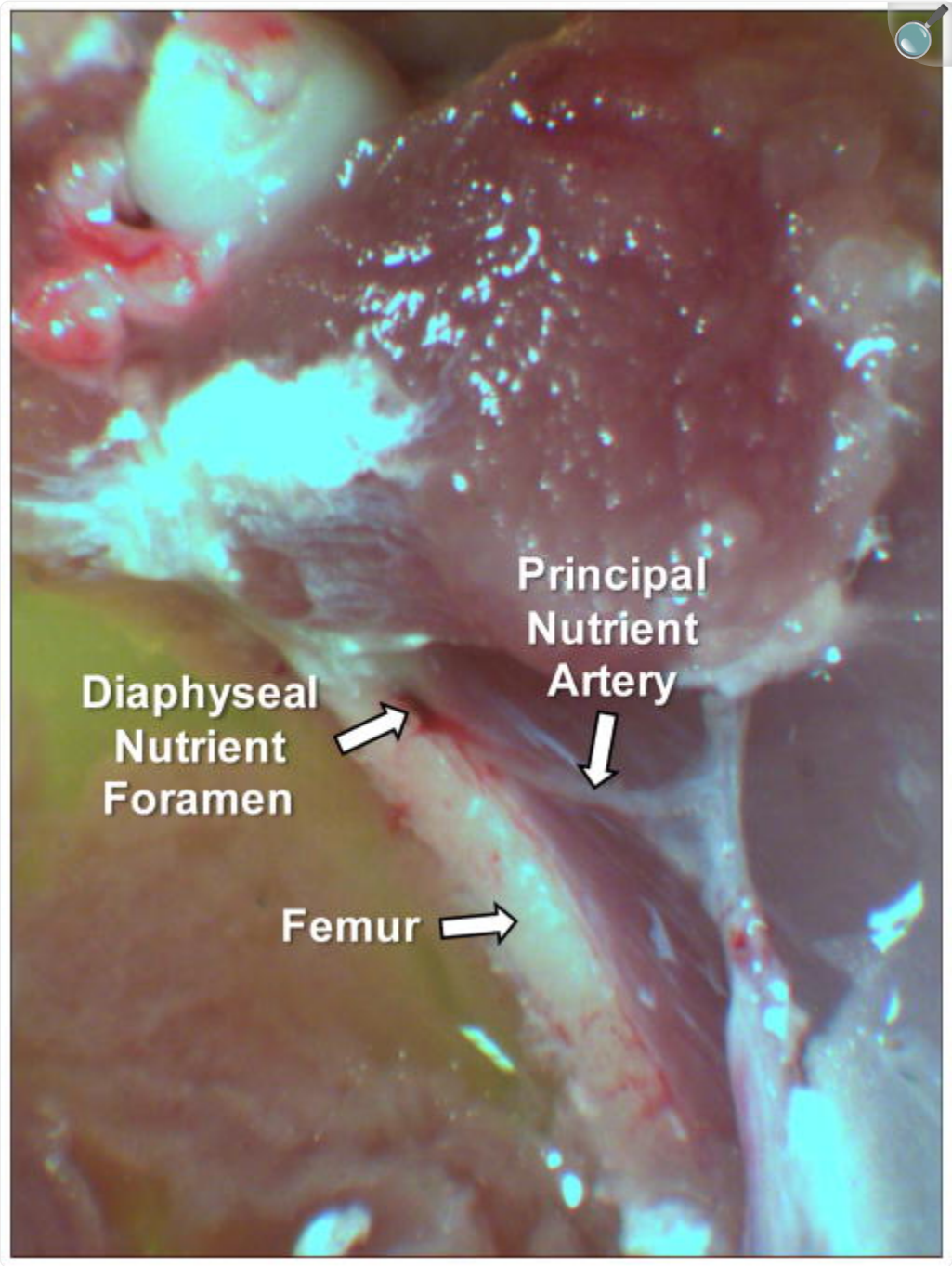

Open in a new tab

Photomicrograph of the rat principal nutrient artery and the diaphyseal nutrient foramen of the right femur.

Histomorphometry

Following determination of maximal diameter and medial wall thickness using videomicroscopy, the cannulated and pressurized arteries were then fixed with a 4% formaldehyde buffer solution, stained with eosin, and embedded in paraffin as previously described [25, 32].

From the paraffin-embedded vessels, 7 μm thick cross-sections were cut, mounted on glass microscope slides and stained with eosin hematoxylin and picrosirius red. Vascular structure was evaluated by measuring vessel media layer cross-sectional area (CSA), inner media perimeter, and media wall thickness. Media wall thickness was measured at six points separated by 60-degree angles and averaged. Vessel radius or diameter was calculated from the inner media perimeter measure. All measurements were made using an image processing and shape analysis system (BioQuant TrueColor Windows, Version 2.0, R&M Biometrics, Nashville, TN) as previously described [25, 32].

Shear Stress and Circumferential Wall Stress Determination

Shear Stress

The shear stress (τ) at the inner surface of the PNA was calculated as:

$$\tau = 4\eta Q/\pi\, r_i{}^3$$

where η is the blood viscosity (0.035 Poise) [33], Q is the blood flow rate (ml/min) to the femoral diaphysis and diaphyseal marrow, and intraluminal radius (r_i) of the PNA was calculated from the measured media inner perimeter [25, 34]. Q was designated as the blood flow rate to the femoral diaphysis and diaphyseal marrow because perfusion of these regions occurs via the PNA in adult rats, whereas the proximal and distal metaphyseal regions are perfused via the epiphyseal and metaphyseal nutrient arteries, respectively [9, 35]. PNA wall shear stress was calculated for three conditions: 1) a control condition using control standing Q and control PNA r_i, 2) an unloading condition using unloaded Q and control PNA r_i to assess shear stress in control PNAs with unloading-induced decrements in flow, and 3) an unloaded condition using Q measures in unloaded femora and PNA r_i from unloaded rats to assess whether vascular remodeling serves to normalize shear stress during unloading.

Circumferential Stress

The circumferential wall stress (σ) of the PNA was calculated as:

$$\sigma = P_a r_i/WT$$

where P_a is the arterial pressure and WT is the medial wall thickness [24, 32]. P_a was measured at the level of the PNA through the caudal artery tail catheter while maintaining the pressure transducer at the approximate level of the PNA. Like that of shear stress, circumferential stress was calculated for 1) a control condition using control standing P_a and control PNA r_i and WT measures, 2) an unloading condition using unloaded P_a and control PNA r_i and WT measures to assess circumferential wall stress in a control PNA when unloading has diminished hindlimb arterial pressure, and 3) an unloaded condition using both P_a and PNA dimensions from unloaded rats to assess whether vascular remodeling serves to normalize circumferential wall stress during unloading.

Data Analysis

A one-way ANOVA was used to compare body and tissue masses and PNA structure and mechanical stresses across conditions. Student-Newman-Keuls method was used as a post hoc test to determine the significances of differences among means. Two-way repeated-measures ANOVAs with pairwise comparisons were used to determine the significance of differences in tissue blood flow, vascular resistance and central hemodynamics within (unloaded vs. standing) and among (Con vs. 7-d HU vs. 14-d HU) factors. All values are presented as the mean ± SE. A $P<0.05$ was required for significance.

RESULTS

Body and Soleus Muscle Mass

Body mass was not different among Con (439 ± 11 g), 7-d HU (425 ± 12 g) and 14-d HU (418 ± 10 g) rats. Soleus muscle mass of 7-d HU (198 ± 13 mg) and 14-d HU (187 ± 8 mg) rats was lower than that of Con animals (269 ± 30 mg). Soleus muscle atrophy in HU rats is characteristic of reduced skeletal muscle weight-bearing activity and confirms the effectiveness of the hindlimb unloading treatment.

Central Hemodynamics

In Con rats, heart rate following 10-min of unloading was higher than that in 7- and 14-d HU rats during the unloaded condition (Table 1). When the animals were reloaded, heart rate was higher in the 7-d HU (451 ± 12 beats/min) and 14-d HU (454 ± 10 beats/min) groups relative to that in the Con rats (427 ± 9 beats/min) during standing. Mean caudal tail arterial pressure was not different between Con and 7-d HU rats during unloading, but it was higher in both groups relative to that in 14-d HU rats (Table 1). During reloading, mean caudal tail artery pressure did not differ among groups (Con, 130 ± 4 mmHg; 7-d HU, 127 ± 4 mmHg; 14-d HU, 128 ± 3 mmHg).

Table 1.

Central hemodynamics and regional femoral blood flows during unloading.

	Control 10-min Unloaded	7-Day Unloaded	14-Day Unloaded
Heart rate, beats/min	463 ± 17	435 ± 10*	428 ± 13*
Caudal tail arterial pressure, mmHg	130 ± 6	125 ± 3	115 ± 5*
Regional blood flow, ml/min/100 g			
Proximal metaphysis	16 ± 3	15 ± 4	13 ± 4
Diaphysis	10 ± 2	10 ± 2	8 ± 1
Diaphyseal marrow	37 ± 8	35 ± 7	28 ± 7
Distal metaphysis	21 ± 3	20 ± 4	18 ± 4

Values are means ± SE; $n = 13$ for control, $n = 11$ for 7-d HU, and $n = 11$ for 14-d HU during the unloaded condition.

*Mean significantly different from control unloaded mean ($P<0.05$).

Skeletal Blood Flow and Vascular Resistance

During unloading, femoral bone and marrow blood flow (Table 1) and vascular resistance did not differ among the three groups. With reloading, blood flow increased in the proximal metaphysis, diaphyseal marrow and distal metaphysis of Con rats, but only increased in the diaphyseal marrow of 7- and 14-d HU rats. During standing, blood flow in 14-d HU rats was lower in all four of the regions of the femur relative to that in Con rats (Fig 2). Likewise, vascular resistance in all regions of the femur was higher in 14-d HU rats during reloading (Fig 3).

Figure 2.

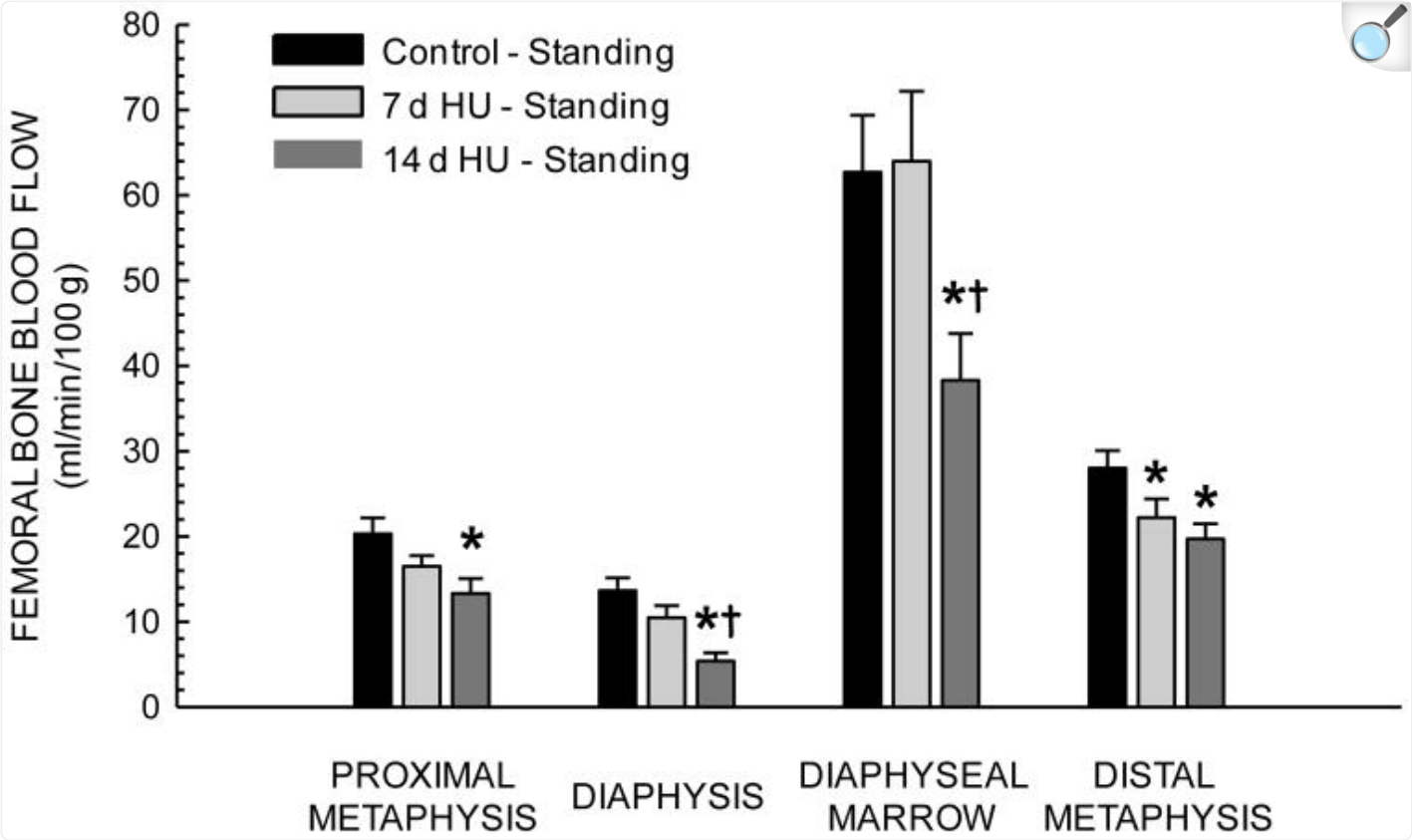

Open in a new tab

Effects of 7 and 14 days of hindlimb unloading (HU) on regional femoral blood flow during standing (reloading). Values are means ± SE. *Mean is different from control standing mean; †mean is different from 7 day unloaded group mean during standing ($P < 0.05$).

Figure 3.

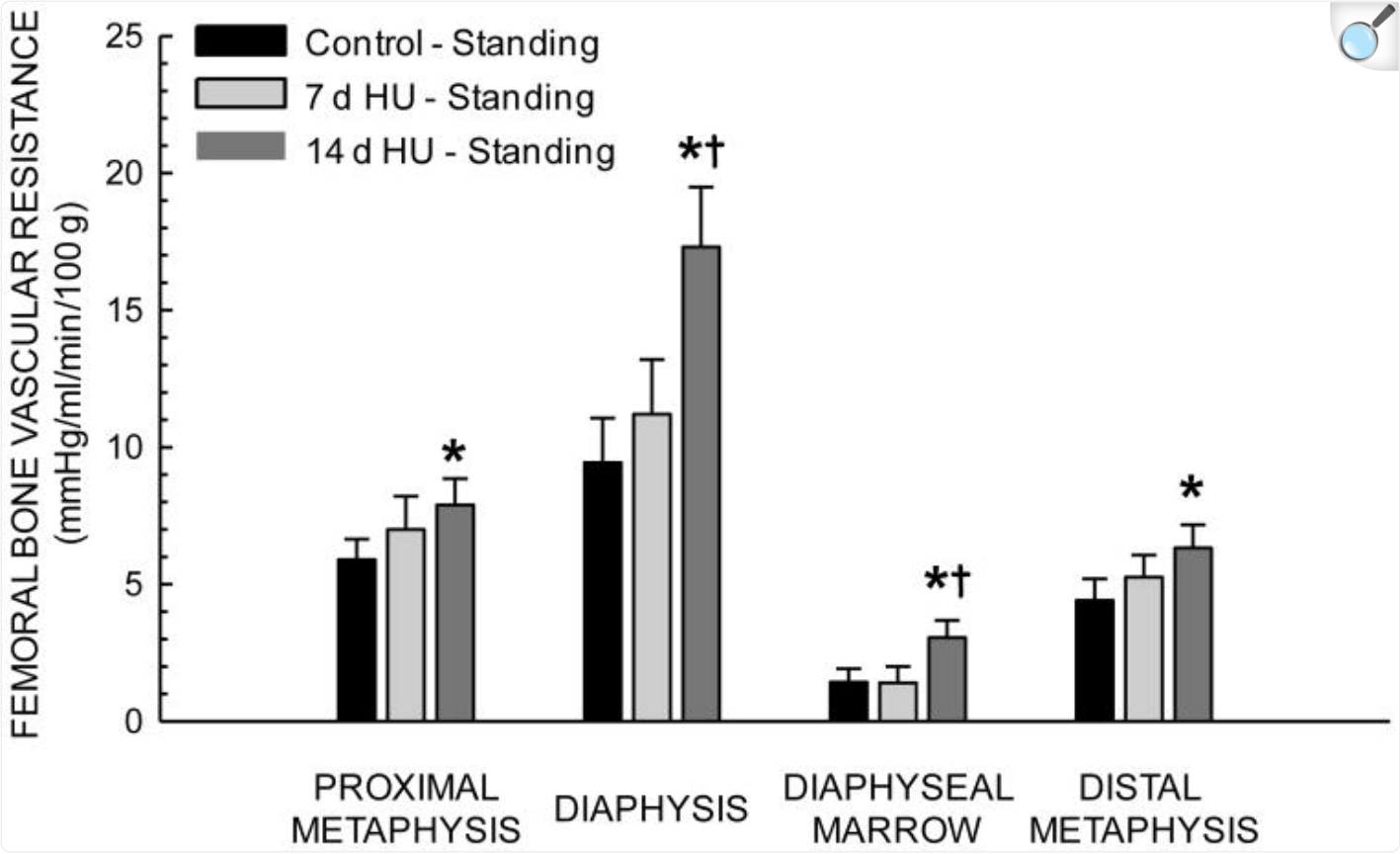

Open in a new tab

Effects of 7 and 14 days of hindlimb unloading (HU) on regional femoral vascular resistances during standing (reloading). Values are means ± SE. *Mean is different from control standing mean; †mean is different from 7 day unloaded group mean during standing ($P < 0.05$).

PNA Structural Characteristics

Chronic skeletal unloading induced a remodeling of the femoral PNA (Fig 4). Using videomicroscopy, maximal intraluminal diameter of PNAs from 14-d HU rats (146 ± 7 μm) was smaller than that from Con rats (177 ± 10 μm). Likewise, PNA medial wall thickness in 14-d HU rats (16 ± 2 μm) was thinner than that from Con animals (22 ± 2 μm). Results derived using histomorphometric techniques were similar to those obtained with videomicroscopy. Intraluminal diameter of PNAs from 14-d HU rats was 15% smaller than that from Con rats and medial wall thickness was 21% thinner in 14-d HU rats (Table 2). The smaller diameters and thinner medial walls resulted in a 23% smaller medial

cross-sectional area in PNAs from 14-d HU animals (Table 2).

Figure 4.

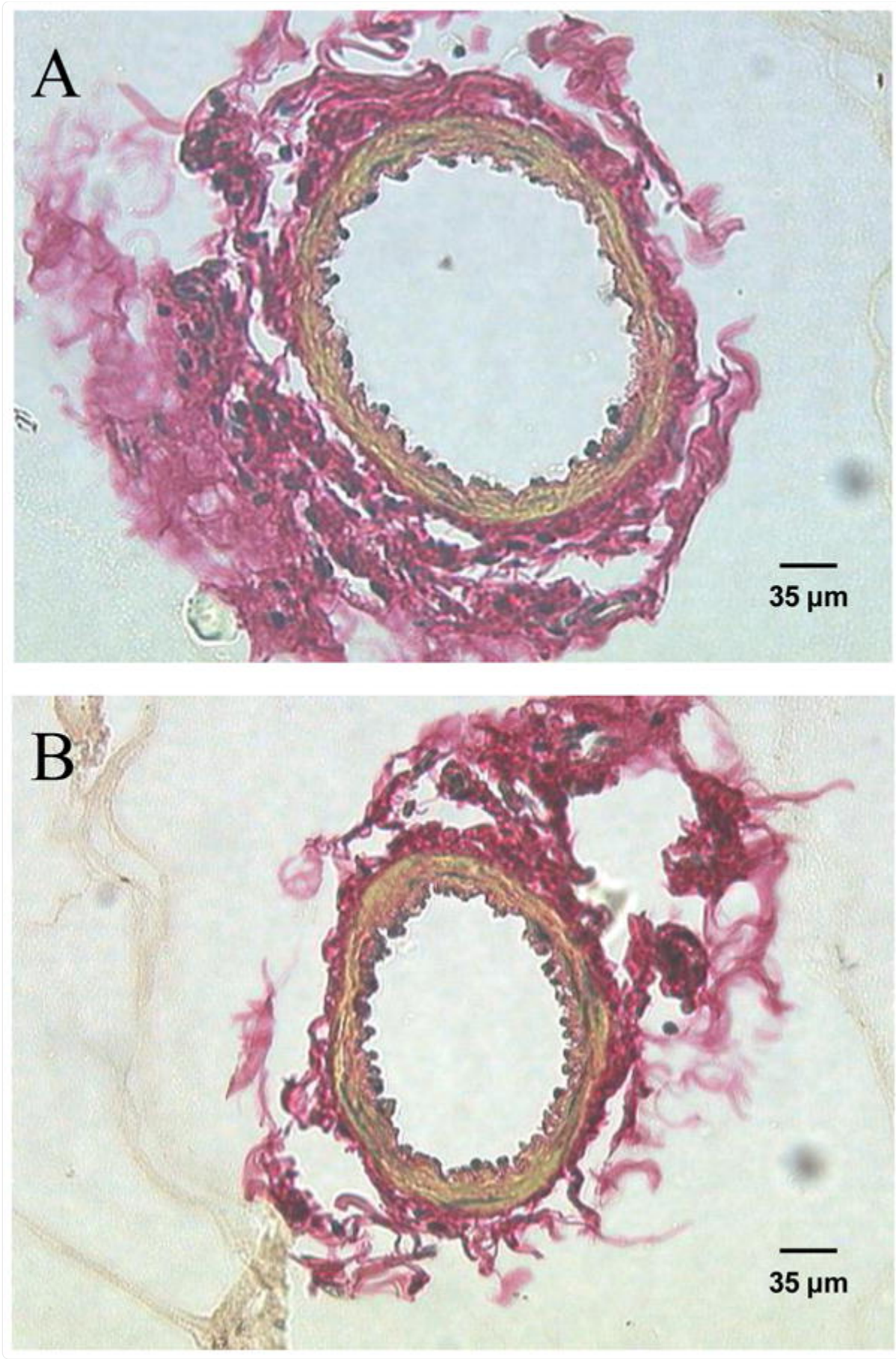

Open in a new tab

Cross-sectional view of femoral principal nutrient arteries from control (A) and 14 day hindlimb unloaded (B) rats. The diameter of the illustrated vessels was closest to the mean diameter of their respective group.

Table 2.

Femoral principal nutrient artery characteristics from histomorphology.

	Control	14-Day Hindlimb Unloaded
Diameter (μm)	162 ± 6	138* ± 5
Medial Wall Thickness (μm)	18.0 ± 0.76	14.3* ± 0.59
Medial Cross-Sectional Area (μm^2)	8,120 ± 272	6,234* ± 232

Open in a new tab

Values are means ± SE; *n*=7 per group.
*Mean significantly different from control mean ($P<0.05$).

PNA Shear Stress and Circumferential Stress

Unloading-induced reductions in blood flow to the femoral diaphysis and marrow resulted in a lower calculated shear stress in the femoral PNA (Fig 5A). However, the remodeling of the PNA to reduce luminal diameter in HU rats (Fig 4) resulted in a similar PNA shear stress in the unloaded condition to that in Con rat PNAs under the control standing condition (Fig 5A).

Figure 5.

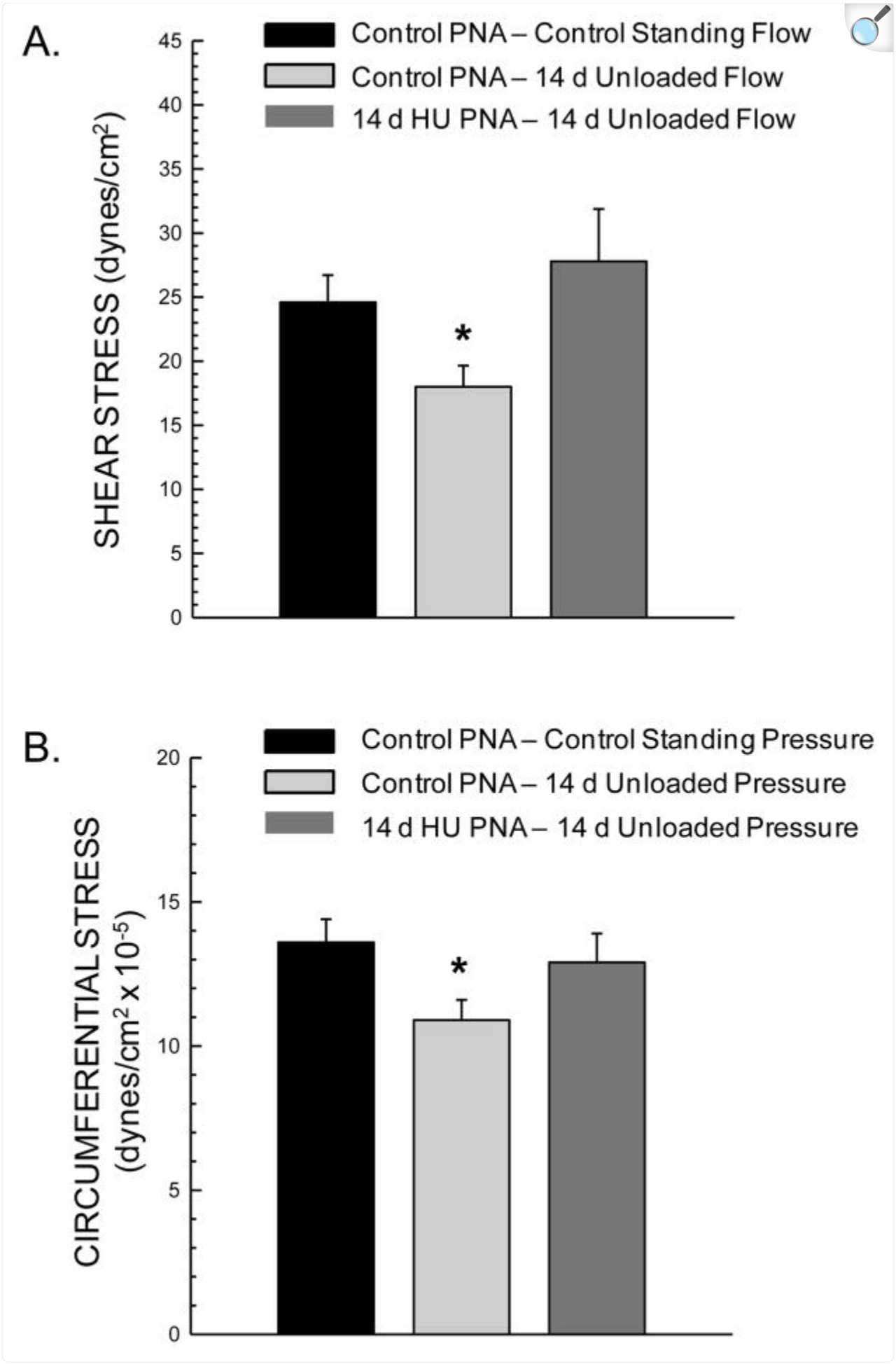
A.
Control PNA – Control Standing Flow
Control PNA – 14 d Unloaded Flow
14 d HU PNA – 14 d Unloaded Flow
SHEAR STRESS (dynes/cm²)
0
5
10
15
20
25
30
35
40
45
*
B.
Control PNA – Control Standing Pressure
Control PNA – 14 d Unloaded Pressure
14 d HU PNA – 14 d Unloaded Pressure
CIRCUMFERENTIAL STRESS
(dynes/cm² x 10⁻⁵)
0
5
10
15
20
*

Open in a new tab

Calculated shear stress (A) and circumferential wall stress (B) in femoral principal nutrient arteries (PNA) of control and hindlimb unloaded (HU) animals during standing. *Mean is different from control standing condition ($P < 0.05$).

The lower arterial pressure in the hindlimb of HU rats during unloading (Table 1) resulted in a lower calculated PNA circumferential wall stress (Fig 5B). This diminished circumferential wall stress was normalized to Con levels through the unloading-induced PNA remodeling to reduce medial wall thickness (Fig 5B).

DISCUSSION

Previous work has shown that as little as 10 min of skeletal unloading reduces bone and marrow perfusion of long bones [6)]. Given that chronic changes in local hemodynamic conditions (e.g., blood flow and arterial pressure) can induce vascular remodeling and impact tissue blood flow capacity [23–25], the purpose of the present investigation was to determine whether 7-d and 14-d of skeletal unloading alters femoral bone and marrow perfusion and vascular resistance during reloading, and to investigate whether putative changes in bone blood flow during reloading are associated with a structural remodeling of the femoral PNA. Results from the present study provide the first evidence that chronic skeletal disuse decreases the bone and marrow hyperemia (Fig 2) and elevates bone vascular resistance (Fig 3) during reloading, as well as induces a remodeling of the bone resistance vasculature. The remodeling of bone resistance arteries (Fig 4) appears to be driven by alterations in mechanical forces within the arterial vasculature that were induced during the unloading treatment, including decreases in blood flow (shear stress, Fig 5A) and hindlimb arterial pressure (circumferential wall stress, Fig 5B). Further, the vascular remodeling served to normalize intraluminal shear stress and circumferential wall stress to levels equivalent to that in control standing rats. While gross structural remodeling of bone resistance arteries occurs to maintain a type of mechanical homeostasis within the artery during unloading (Fig 5), these changes in arterial structure may have adverse consequences with reloading. For example, the structural narrowing of the resistance vasculature could function to limit bone and marrow blood flow capacity and contribute to the elevations in vascular resistance during reloading.

Previous studies have also provided evidence that vascular remodeling occurs within bone during prolonged disuse. For example, Doty et al. [36] reported that the vascular space (area) in the diaphyseal region of the tibia in rats flown 12.5 days in space on a Cosmos biosatellite tended to be lower than that in ground control animals. The lack of statistical significance was attributed to the low number of animals studied ($n = 5$ per group). Fei et al. (17) have also demonstrated small vessel rarefaction in the tibial metaphysis of 21-d HU rats using a technique to quantify microvascular network structure that does not differentiate between arteries, veins and capillaries or include larger

microvessels of the size of resistance arteries [37]. And using sciatic neurectomy to generate unilateral disuse in the rat hindlimb, Matsumoto et al. [38] investigated disuse effects on the pervasive canal network in cortical bone of the tibia during growth. This canal network provides the infrastructure for vascular distribution throughout bone. Fourteen wks of disuse decreased canal number and density, as well as diminishing periosteal and endocortical bone formation. The authors speculated that the less dense canal network would be accompanied by a lower perfusion rate [38], which could adversely affect the fluid pressure gradient and fluid flow between the endosteal vasculature and periosteal lymphathics [39, 40]. An active transmural pressure gradient and fluid flow is rudimentary to the bone formation process [8]. Collectively, these studies suggest several types of unloading-induced vascular adaptations in bone: 1) a narrowing of bone resistance arteries [present study], which could negatively impact the bulk flow of oxygen and nutrients into bone, cellular transport, and ultimately the bulk fluid flow through capillaries into the interstitial spaces [9, 10, 35], and 2) rarefaction of the bone microvascular network and supporting infrastructure [17, 36, 38], which among other things could impair potential signaling between the vascular endothelium and bone remodeling units [11, 14–16].

The consequences of insufficient perfusion of bone and marrow during loading could be severe. Ischemic bone is susceptible to several deleterious effects, including loss of osteocytes [41] and diminished osteoblast activity [42]. Interestingly, osteoclast activity is seemingly unperturbed by similar decrements in blood supply [42]. McCarthy [43] has suggested that hypoxia produced by inadequate blood flow would be accompanied by slight decreases in pH, which could serve to stimulate osteoclast activity. Bone marrow ischemia is also a precursor to osteonecrosis [44]. Although there is no evidence that unloading-induced decrements in blood flow during reloading are severe enough to provoke osteonecrosis, an underperfusion of bone and marrow could have adverse effects on bone structure and health, particularly if the energetic requirements of metabolically active bone cells exceed the capacity of the vasculature to provide sufficient delivery of oxygen and nutrients. Additionally, under such low-flow conditions there may be a diminished influence of systemic factors on bone tissue and a concomitant increase in the dependency and influence of local factors in bone.

The classic theory of vascular remodeling holds that it is stimulated by local hypoxemia [45, 46]. While still an important factor, hypoxia may not be the direct impetus for alterations in vascular structure. Rather, it appears that arteries respond to changes in mechanical stress and strain by remodeling their gross structural properties in order to maintain a type of mechanical homeostasis [23]. In conduit arteries, for example, structure is maintained by “normal” blood flow (shear stress) and “normal” arterial pressure (circumferential wall stress) [23, 46]. Deviations from this hemodynamic status quo are critical mechanisms to induce vascular remodeling [45, 46]. For instance, research on large conduit arteries reveals that decreases in blood flow through the artery reduces wall shear stress, and this induces a remodeling that diminishes luminal diameter and correspondingly serves to normalize wall shear stress [22]. Likewise, hypertension increases the circumferential wall stress of arteries and elicits an adaptive thickening of the media layer of the arterial wall that consequently serves to lower circumferential wall stress [23].

Much of what is known regarding the mechanisms that induce vascular remodeling has come from studies of conduit

arteries exposed to increases and decreases in blood flow or increases in arterial pressure [23, 24, 45, 46]. Large conduit arteries, however, are not subjected to the same physical or chemical environment (e.g., altered tissue oxygenation and local pH) of small resistance arteries within tissue. Only a relatively small number of studies have investigated the remodeling of resistance arteries and few of these contain measures necessary to determine changes in resistance artery shear stress or circumferential wall stress. To our knowledge, the present study is the first to examine the effects of changes in the hydrodynamic mechanical environment on the bone vasculature. Although the bone vasculature is unique in many ways [9, 10, 35, 43, 44], the results demonstrate that bone resistance arteries also remodel to maintain a mechanical homeostasis during conditions of prolonged disuse and unloading (Fig 5A & 5B). The structural modification of the femoral PNA to decrease wall thickness in response to chronic reductions in hindlimb arterial pressure could make the vessels more susceptible to degeneration or disruption of the vascular wall, as was observed to occur in the tibia of spaceflown rats following 2-d of reloading [36]. Likewise, the narrowing of the PNA maximal intraluminal diameter in response to the chronic unloading-induced decreases in blood flow could impose a structural limitation on oxygen and nutrient delivery to the bone and marrow upon return to weight bearing activity.

In conclusion, results from the present study confirm previous observations [6] that skeletal unloading decreases long bone blood flow (Table 1). The results further demonstrate that this prolonged skeletal disuse impairs the ability of the vasculature to augment bone and marrow blood flow upon reloading (Fig 2). The diminished hyperemic response is the result of elevations in vascular resistance within the bone and marrow (Fig 3) and is associated with a remodeling of the resistance vasculature (Fig 4). This arterial remodeling served to maintain shear stress (Fig 5A) and circumferential wall stress (Fig 5B) through decreases in maximal diameter and medial wall thickness, respectively, in the face of a diminished blood flow and hindlimb arterial pressure. The functional consequences of the structural narrowing of resistance arteries in particular could serve to limit bone and marrow blood flow capacity and possibly contribute to bone ischemia during reloading or physical activity.

Highlights.

- Chronic skeletal unloading decreases bone and marrow blood flow (BF) to the femur
- Reloading results in a lower bone and marrow BF and higher vascular resistance (VR)
- The lower BF is associated with vascular remodeling in the femur
- The vascular remodeling is driven by alterations in intravascular mechanical forces
- This remodeling also limits bone BF capacity and elevates VR during reloading

Acknowledgments

This study was supported by National Aeronautics and Space Administration Grant NNX12AL41G.

Footnotes

References

1. Bloomfield SA, Allen MR, Hogan HA, Delp MD. Site- and compartment-specific changes in bone with hindlimb unloading in mature adult rats. Bone. 2002;31:149–157. doi: 10.1016/s8756-3282(02)00785-8. [DOI] [PubMed] [Google Scholar]

2. Dehority W, Halloran BP, Bikle DD, Curren T, Kostenuik PJ, Wronski TJ, Shen Y, Rabkin B, Bouraoui A, Morey-Holton E. Bone and hormonal changes induced by skeletal unloading in the mature male rat. Am J Physiol Endocrinol Metab. 1999;276:E62–E69. doi: 10.1152/ajpendo.1999.276.1.e62. [DOI] [PubMed] [Google Scholar]

3. Globus RK, Bikle DD, Halloran BP, Morey-Holton E. Skeletal response to dietary calcium in a rat model simulating weightlessness. J Bone Miner Res. 1986;1:191–197. doi: 10.1002/jbmr.5650010205. [DOI] [PubMed] [Google Scholar]

4. Roer RD, Dillaman RM. Bone growth and calcium balance during simulated weightlessness in the rat. J Appl Physiol. 1990;68:13–20. doi: 10.1152/jappl.1990.68.1.13. [DOI] [PubMed] [Google Scholar]

5. Bergula AP, Huang W, Frangos JA. Femoral vein ligation increases bone mass in the hindlimb suspended rat. Bone. 1999;24:171–177. doi: 10.1016/s8756-3282(98)00165-3. [DOI] [PubMed] [Google Scholar]

6. Colleran PN, Wilkerson MK, Bloomfield SA, Suva LJ, Turner RT, Delp MD. Alterations in skeletal perfusion with simulated microgravity: A possible mechanism for bone remodeling. J Appl Physiol. 2000;89:1046–1054. doi: 10.1152/jappl.2000.89.3.1046. [DOI] [PubMed] [Google Scholar]

7. Turner CH. Site-specific skeletal effects of exercise: Importance of interstitial fluid pressure. Bone. 1999;24:161–162. doi: 10.1016/s8756-3282(98)00184-7. [DOI] [PubMed] [Google Scholar]

8. Turner CH, Forwood MR, Otter MW. Mechanotransduction in bone: do bone cells act as sensors of fluid

flow? FASEB J. 1994;8:875–878. doi: 10.1096/fasebj.8.11.8070637. [DOI] [PubMed] [Google Scholar]

9. Brookes M, Revell WJ. Blood Supply of Bone: Scientific Aspects. Springer-Verlag; New York, NY, USA: 1998. [Google Scholar]

10. Kelly P. Pathways of transport in bone. In: Sheppard JT, Abboud FM, editors. The Handbook of Physiology: The Cardiovascular System III. Williams & Wilkins; Baltimore, MD, USA: 1983. pp. 371–396. [Google Scholar]

11. Collin-Osdoby P. Role of vascular endothelial cells in bone biology. J Cell Biochem. 1994;55:304–309. doi: 10.1002/jcb.240550306. [DOI] [PubMed] [Google Scholar]

12. Dominguez JM, Prisby RD, Muller-Delp JM, Allen MR, Delp MD. Increased nitric oxide-mediated vasodilation of bone resistance arteries is associated with increased trabecular bone volume after endurance training in rats. Bone. 2010;46:813–819. doi: 10.1016/j.bone.2009.10.029. [DOI] [PMC free article] [PubMed] [Google Scholar]

13. Judex S, Gross TS, Bray RC, Zernicke RF. Adaptation of bone to physiological stimuli. J Biomech. 1997;30:421–429. doi: 10.1016/s0021-9290(96)00060-7. [DOI] [PubMed] [Google Scholar]

14. Parfitt AM. The mechanism of coupling: A role for the vasculature. Bone. 2000;26:319–323. doi: 10.1016/S8756-3282(00)80937-0. [DOI] [PubMed] [Google Scholar]

15. Prisby RD, Ramsey MW, Behnke BJ, Dominguez JM, Donato AJ, Allen MR, Delp MD. Aging reduces skeletal blood flow, endothelium-dependent vasodilation and nitric oxide bioavailability in rats. J Bone Miner Res. 2007;22:1280–1288. doi: 10.1359/jbmr.070415. [DOI] [PubMed] [Google Scholar]

16. Prisby RD, Dominguez JM, Muller-Delp JM, Allen MR, Delp MD. Aging and estrogen status: A possible endothelium-dependent vascular coupling mechanism in bone remodeling. PLoS ONE. 2012;7:e48564. doi: 10.1371/journal.pone.0048564. [DOI] [PMC free article] [PubMed] [Google Scholar]

17. Fei J, Peyrin F, Malaval L, Vico L, Lafage-Proust MH. Imaging and quantitative assessment of long bone vascularization in the adult rat using microcomputed tomography. Anat Rec. 2010;293:215–224. doi: 10.1002/ar.21054. [DOI] [PubMed] [Google Scholar]

18. Arnaud SB, Posell MR, Whalen RT, Vernikos-Danellis J. Bone mineral redistribution during head down tilt bed rest (Abstract) ASGSB Bull. 1989;2:54. [Google Scholar]

19. Leblanc AD, Schneider VS, Evans HJ, Engelbretson DA, Krebs JM. Bone mineral loss and recovery after 17 weeks of bed rest. J Bone Miner Res. 1990;5:843–850. doi: 10.1002/jbmr.5650050807. [DOI] [PubMed] [Google Scholar]

20. Laroche M, Moulinier L, Leger P, Lefebvre D, Mazieres B, Boccalon H. Bone mineral decrease in the leg with unilateral chronic occlusive arterial disease. Clin Exp Rheumatol. 2003;21:103–106. [PubMed] [Google Scholar]

21. Brownlee RD, Langille BL. Arterial adaptations to altered blood flow. Can J Physiol Pharmacol. 1991;69:978–983. doi: 10.1139/y91-147. [DOI] [PubMed] [Google Scholar]

22. Langille BL, O'Donnell F. Reductions in arterial diameter produced by chronic decreases in blood flow are endothelium-dependent. Science. 1986;231:405–407. doi: 10.1126/science.3941904. [DOI] [PubMed] [Google Scholar]

23. Humphrey JD. Mechanisms of arterial remodeling in hypertension: couples roles of wall shear and intramural stress. Hyperten. 2008;52:195–200. doi: 10.1161/HYPERTENSIONAHA.107.103440. [DOI] [PMC free article] [PubMed] [Google Scholar]

24. Humphrey JD. Cardiovascular Solid Mechanics: Cells, Tissues, and Organs. Springer-Verlag; New York, NY, USA: 2002. [Google Scholar]

25. Delp MD, Colleran PC, Wilkerson MK, McCurdy MR, Muller-Delp J. Structural and functional remodeling of skeletal muscle microvasculature is induced by simulated microgravity. Am J Physiol Heart Circ Physiol. 2000;278:H1866–H1873. doi: 10.1152/ajpheart.2000.278.6.H1866. [DOI] [PubMed] [Google Scholar]

26. McDonald KS, Delp MD, Fitts RH. Effect of hindlimb unweighting on tissue blood flow in the rat. J Appl Physiol. 1992;72:2210–2218. doi: 10.1152/jappl.1992.72.6.2210. [DOI] [PubMed] [Google Scholar]

27. Delp MD, Armstrong RB. Blood flow in normal and denervated muscle during exercise in conscious rats. Am J Physiol Heart Circ Physiol. 1988;255:H1509–H1515. doi: 10.1152/ajpheart.1988.255.6.H1509. [DOI] [PubMed] [Google Scholar]

28. Meininger G, Harris P, Joshua I. Distributions of microvascular pressure in skeletal muscle of one- kidney, one clip, two-kidney, one clip, and deoxycorticosterone-salt hypertensive rats. Hyperten. 1984;6:27–34. doi: 10.1161/01.hyp.6.1.27. [DOI] [PubMed] [Google Scholar]

29. Behnke BJ, Stabley JN, McCullough DJ, Davis RT, III, Dominguez JM, II, Muller-Delp JM, Delp MD. Effects of spaceflight and ground recovery on mesenteric artery and vein constrictor properties in mice. FASEB J. 2013;27:399–409. doi: 10.1096/fj.12-218503. [DOI] [PMC free article] [PubMed] [Google Scholar]

30. Colleran PN, Behnke BJ, Wilkerson MK, Donato AJ, Delp MD. Simulated microgravity alters rat mesenteric artery vasoconstrictor dynamics through an intracellular Ca2+ release mechanism. Am J Physiol

Reg Int Comp Physiol. 2008;294:R1577–R1585. doi: 10.1152/ajpregu.00084.2008. [DOI] [PubMed] [Google Scholar]

31. Taylor CR, Hanna M, Behnke BJ, Stabley JN, McCullough DJ, Davis RT, III, Ghosh P, Papadopoulos A, Muller-Delp JM, Delp MD. Spaceflight-induced alterations in cerebral artery vasoconstrictor, mechanical, and structural properties: implications for elevated cerebral perfusion and intracranial pressure. FASEB J. 2013;27:2282–2292. doi: 10.1096/fj.12-222687. [DOI] [PMC free article] [PubMed] [Google Scholar]

32. Wilkerson MK, Muller-Delp J, Colleran PN, Delp MD. Effects of hindlimb unloading on rat cerebral, splenic, and mesenteric resistance artery morphology. J Appl Physiol. 1999;87:2115–2121. doi: 10.1152/jappl.1999.87.6.2115. [DOI] [PubMed] [Google Scholar]

33. Lipowsky HH. Shear stress in the circulation. In: Belvan JA, Kaley G, Rubanyi GM, editors. Flow-Dependent Regulation of Vascular Function. New York: Oxford University Press; 1995. pp. 28–45. [Google Scholar]

34. Rachev A, Stergiopulos N, Meister JJ. A model for geometric and mechanical adaptation of arteries to sustained hypertension. J Biomech Engineer. 1998;120:9–17. doi: 10.1115/1.2834313. [DOI] [PubMed] [Google Scholar]

35. Brookes M. An anatomy of the osseous circulation. Bone. 1986;3:32–35. [Google Scholar]

36. Doty SB, Morey-Holton ER, Durnova GN, Kaplansky AS. Cosmos 1887: morphology, histochemistry, and vasculature of the growing rat tibia. FASEB J. 1990;4:16–23. doi: 10.1096/fasebj.4.1.2153083. [DOI] [PubMed] [Google Scholar]

37. Roche B, David V, Vanden-Bossche A, Peyrin F, Malaval L, Vico L, Lafage-Proust MH. Structure and quantification of microvascularisation within mouse long bones: What and how should we measure? Bone. 2012;50:390–399. doi: 10.1016/j.bone.2011.09.051. [DOI] [PubMed] [Google Scholar]

38. Matsumoto T, Yoshino M, Uesugi K, Tanaka M. Biphasic change and disuse-mediated regression of canal network structure in cortical bone of growing rats. Bone. 2007;41:239–246. doi: 10.1016/j.bone.2007.04.192. [DOI] [PubMed] [Google Scholar]

39. Dillaman RM, Roer RD, Gay DM. Fluid movement in bone: theoretical and empirical. J Biomech. 1991;24(Suppl 1):163–177. doi: 10.1016/0021-9290(91)90386-2. [DOI] [PubMed] [Google Scholar]

40. Reich KM, Frangos JA. Effect of flow on prostaglandin E2 and inositol trisphosphate levels in osteoblasts. Am J Physiol. 1991;261:C428–C432. doi: 10.1152/ajpcell.1991.261.3.C428. [DOI] [PubMed] [Google Scholar]

41. Catto M. Ischaemia of bone. J Clin Pathol. 1977;11(Suppl):78–93. doi: 10.1136/jcp.s3-11.1.78. [DOI] [PMC free article] [PubMed] [Google Scholar]

42. Barou O, Mekraldi S, Vico L, Boivin G, Alexandre C, Lafage-Proust MH. Relationships between trabecular bone remodeling and bone vascularization: a quantitative study. Bone. 2002;30:604–612. doi: 10.1016/s8756-3282(02)00677-4. [DOI] [PubMed] [Google Scholar]

43. McCarthy I. The physiology of bone blood flow: a review. J Bone Joint Surg Am. 2006;88(Suppl 3):4–9. doi: 10.2106/JBJS.F.00890. [DOI] [PubMed] [Google Scholar]

44. Laroche M. Intraosseous circulation from physiology to disease. Joint Bone Spine. 2002;69:262–269. doi: 10.1016/s1297-319x(02)00391-3. [DOI] [PubMed] [Google Scholar]

45. Hänze J, Weissmann N, Grimminger F, Seeger W, Rose F. Cellular and molecular mechanisms of hypoxia-inducible factor driven vascular remodeling. Thromb Haemost. 2007;97:774–787. [PubMed] [Google Scholar]

46. Prior BM, Lloyd PG, Yang HT, Terjung RL. Exercise-induced vascular remodeling. Exerc Sport Sci Rev. 2003;31:26–33. doi: 10.1097/00003677-200301000-00006. [DOI] [PubMed] [Google Scholar]